

Differences in Visible and Near-IR Responses, and Derived Vegetation Indices, for the NOAA-9 and NOAA-10 AVHRRs: A Case Study

K. P. Gallo*

Satellite Research Laboratory, NOAA/NESDIS, Washington, DC 20233

J. C. Eidenshink

T. G. S. Technology, Inc., EROS Data Center, Sioux Falls, SD 57198

ABSTRACT: This study evaluates the differences in the visible and near-IR responses of the Advanced Very High Resolution Radiometers (AVHRR) of the National Oceanic and Atmospheric Administration (NOAA)-9 and -10 satellites for coincident sample locations. The study also evaluates the differences in vegetation indices computed from those data. Data were acquired of the southeast portion of the United States for the 6 December 1986 daylight orbits of NOAA-9 and NOAA-10 satellites. The data sets were registered and 38 coincident sample locations were selected that included land and water surfaces. The data were calibrated to reflectance values with coefficients supplied by NOAA. The visible and near-IR reflectance values and the derived vegetation index values of the NOAA-9 AVHRR were usually greater than those of the NOAA-10. Visible and near-IR reflectance values exhibited trends that appeared to be related to the satellite scan angles at the examined sample locations. Linear relationships were developed between the vegetation indices of the two systems. The vegetation index values for the NOAA-9 and NOAA-10 AVHRR displayed nearly constant differences for a variety of surface features. The results suggest that, with appropriate gain and offset, the vegetation indices of the two sensor systems may be interchangeable for assessment of land surfaces.

INTRODUCTION

THE USE OF SATELLITES to monitor land surface features has increased with the near daily coverage of most Earth locations by the NOAA series of satellites. The advanced very high resolution radiometer (AVHRR) on the NOAA series of satellites provides a nadir pixel resolution of 1.1 km (Kidwell, 1986). While this resolution is not as fine as that of the Landsat multispectral scanner (MSS) or thematic mapper (TM) or the System Probatoire d'Observation de la Terre (SPOT) sensors, its near daily coverage of most locations on the Earth's surface has made the AVHRR system quite useful to the research community (e.g., Justice, 1986). The visible and near-IR bands of the AVHRR are often utilized, by individuals interested in land surface features, to compute the normalized difference (ND) vegetation index: i.e.,

$$ND = (\text{near-IR} - \text{visible}) / (\text{near-IR} + \text{visible}).$$

Ground-based field experiments have demonstrated that several agriculturally important variables are related to the ND and other combinations of two or more wavebands in the visible and near-IR. Agronomic variables related to these vegetation indices include leaf area index (Asrar *et al.*, 1984; Daughtry *et al.*, 1983; Dusek *et al.*, 1985; Gallo and Daughtry, 1987; Gardner *et al.*, 1985; Hatfield *et al.*, 1985; Hinzman *et al.*, 1986), the photosynthetically active radiation absorbed by a crop canopy (Asrar *et al.*, 1984; Gallo *et al.*, 1985; Hatfield *et al.*, 1984), and wet and/or dry phytomass (Dusek *et al.*, 1985; Gardner *et al.*, 1985; Hinzman *et al.*, 1986). The ND vegetation index is often utilized to minimize the influence of illumination and atmospheric conditions that may vary from day to day or over longer intervals (Tarpley *et al.*, 1984). Weekly, or longer, composites of satellite derived ND (Holben, 1986; Tarpley *et al.*, 1984) have been used to classify land-cover types (Tucker *et al.*, 1985), monitor seasonal fluctuations in the extent of vegetation (Goward *et al.*, 1985; Justice *et al.*, 1985; Schneider *et al.*, 1985), and monitor

monthly variations in globally averaged atmospheric CO₂ (Tucker *et al.*, 1986).

Studies that utilize NOAA AVHRR data have primarily relied on data acquired after local noon. These studies utilize the NOAA satellites assigned an odd number, e.g., NOAA-9, which designates the satellite as one that has a northbound Equator crossing time of approximately 1430 local solar time. The development of clouds in the afternoon hours, due to radiational heating, often precludes daily observations of many land surfaces with the odd-numbered NOAA satellites. The early morning orbit (southbound Equator crossing time of approximately 0730 local solar time) of the NOAA-10 (or other even-numbered) satellite may, when solar elevation angles permit, provide an opportunity for observation of land surfaces usually obscured by clouds at the time of the afternoon satellite orbit. The use of data acquired with both odd- and even-numbered satellites to assess or monitor specific surface features would be advantageous due to the increased probability of data uncontaminated with clouds.

There are slight differences, among the past and current AVHRR instruments, between their visible (band 1) and near-IR (band 2) wavebands and the response of the sensors within these wavebands. Bands 1 and 2 of the NOAA-9 and NOAA-10 AVHRR's have bandwidths, based on 50 percent relative response, of 570 to 700 and 715 to 982 nm, and 573 to 684 and 723 to 981 nm, respectively. The primary difference between the satellites, however is their different orbital characteristics. On any single day, a specific site on the ground would likely be viewed under different conditions by the NOAA-9 compared to NOAA-10 satellite. The observations would likely include different satellite scan angles, satellite azimuth angles with respect to the target, and solar elevation and azimuth angles. Additionally, the two sets of observations would most likely be made under different atmospheric conditions. Several of the effects of off-nadir views, and the increased influence of the atmosphere associated with these views, on the red and near-IR wavebands, and normalized difference vegetation index, of the AVHRR have been simulated (Holben and Fraser, 1984; Holben *et al.*, 1986) and observed (Brown *et al.*, 1982; Duggin *et al.*, 1982; Taylor *et al.*, 1985).

* Currently a participant in the Cooperative Federal Land Remote Sensing Research Program, EROS Data Center, Sioux Falls, SD 57198.

Atmospheric conditions may also introduce additional variability in the vegetation indices computed with data from different sensors (Jackson *et al.*, 1983).

The objective of this study was to examine the differences in the visible and near-IR waveband responses of the NOAA-9 and NOAA-10 AVHRR data acquired for coincident sample locations. Differences in vegetation indices between the two systems are also evaluated. If the visible, near-IR, or vegetation index responses for the two AVHRR sensors are highly related, then the data acquired with one sensor may be used to model the data unavailable from the normally utilized satellite.

MATERIALS AND METHODS

DATA ACQUISITION AND ANALYSIS

Data were acquired of the southeast portion of the United States for the 6 December 1986 daylight orbits of NOAA-9 and NOAA-10 satellites. These data were selected because they were acquired for a similar area with nearly cloud-free conditions over a large portion of the area. The near-coincident area of data acquisition for the two satellites, with nearly cloud free conditions, is a relatively unique occurrence. Times of orbit overpass along the nadir paths were approximately 1541 and 0842 (UT) for the NOAA-9 and NOAA-10 satellites, respectively. The NOAA-9 image was geometrically registered and resampled to a one-kilometer grid Mercator projection using cubic convolution (Young and Fahle, 1981). The NOAA-10 image was registered to the NOAA-9 image with an RMSE of 0.5 pixels. A total of 38 coincident sample locations along two transects were selected for analysis (Figure 1). The sample locations included land and water surfaces. The effects of any possible ground tracking variations between the satellites, and differences in original pixel size due to the scan angles, were minimized through the identification of a three- by three-pixel window that surrounded each initially selected sample location. The mean value of the visible and near-IR response of each three by three window was computed and utilized in the analysis of this study.

The satellite visible and near-IR data of the NOAA-9 and NOAA-10 AVHRR systems were calibrated to reflectance (often cited as "albedo") values with the coefficients supplied with the data by NOAA (Kidwell, 1986). The normalized difference vegetation index was computed from the data of each satellite for each sample location. Solar zenith and azimuth angles at each of the sample locations were computed as were satellite scan and azimuthal angles. The data were examined for the influence on

the different solar and satellite orbital characteristics on the visible, near-IR, and vegetation index values for the range of sample locations.

The characteristics of the land surface features included in this study were not directly examined. The sample locations included primarily forests and cropland (U.S. Department of Agriculture, Soil Conservation Service, 1981) and water.

Visual examination of displayed images of the acquired visible and near-IR data of both satellites was used to select the sample locations and verify cloud-free conditions. Sky cover data near the times of satellite orbit over the southeast U.S. were obtained from the National Climatic Data Center* of NOAA to supplement the visual verification of clear sky conditions over the sample locations.

RESULTS AND DISCUSSION

SOLAR AND SATELLITE GEOMETRY

The nadir paths and times of orbits of the two satellites result in a variety of satellite and solar geometric differences between the data acquired with NOAA-9 compared to NOAA-10. The nadir paths of the two satellites (Figure 1) result in a near nadir view (scan angle of nearly 0 degrees) of sample location 6 with the NOAA-10 AVHRR (Figure 2). The scan angles of both satellite systems increased to a maximum at location 27. Scan angles for NOAA-9 increased from locations 1 to 27. A positive scan angle (Figure 2), as utilized in this study, denotes a scan in an easterly direction. Scan angles along the southern transect (not shown) varied less for both satellites, compared to the northern transect. The range of scan angles along the southern transect varied less, compared to the northern transect, as the southern transect is nearer to the nadir path of both satellites, and the southern transect is less than that of the northern transect (Figure 1).

Satellite azimuth angle, the angle from which the satellite views the sample location, varies as a result of the location of the nadir path. Locations 1 through 27 were viewed by NOAA-9 (Figure 2) from the west. Locations 1 through 6 were viewed by NOAA-10 from the east while locations 7 through 27 are viewed from the west. Locations 28 and 29 on the southern transect were viewed by NOAA-9 from the east, while locations 30 through

* National Climatic Data Center, NOAA/NESDIS, Federal Building, Asheville, NC 28801

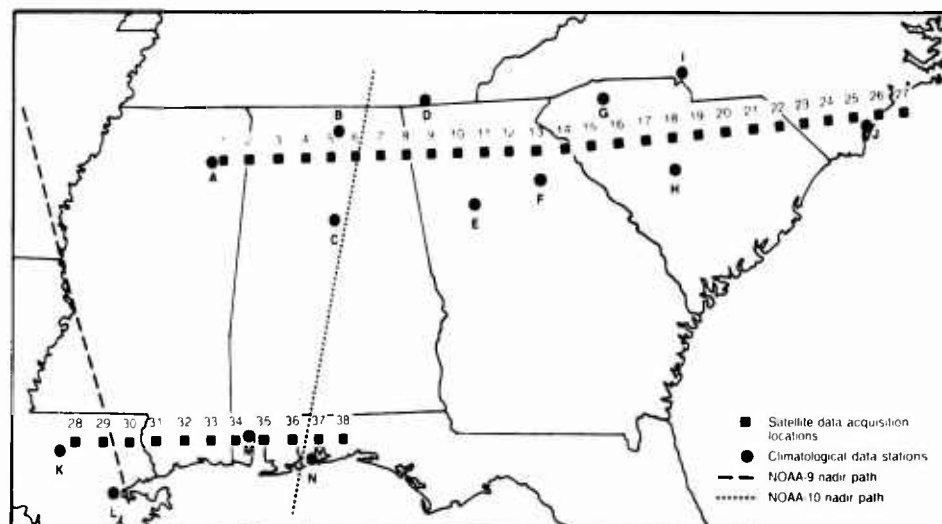


FIG. 1. Selected sample locations, satellite nadir paths, and climatological data stations included in the study.

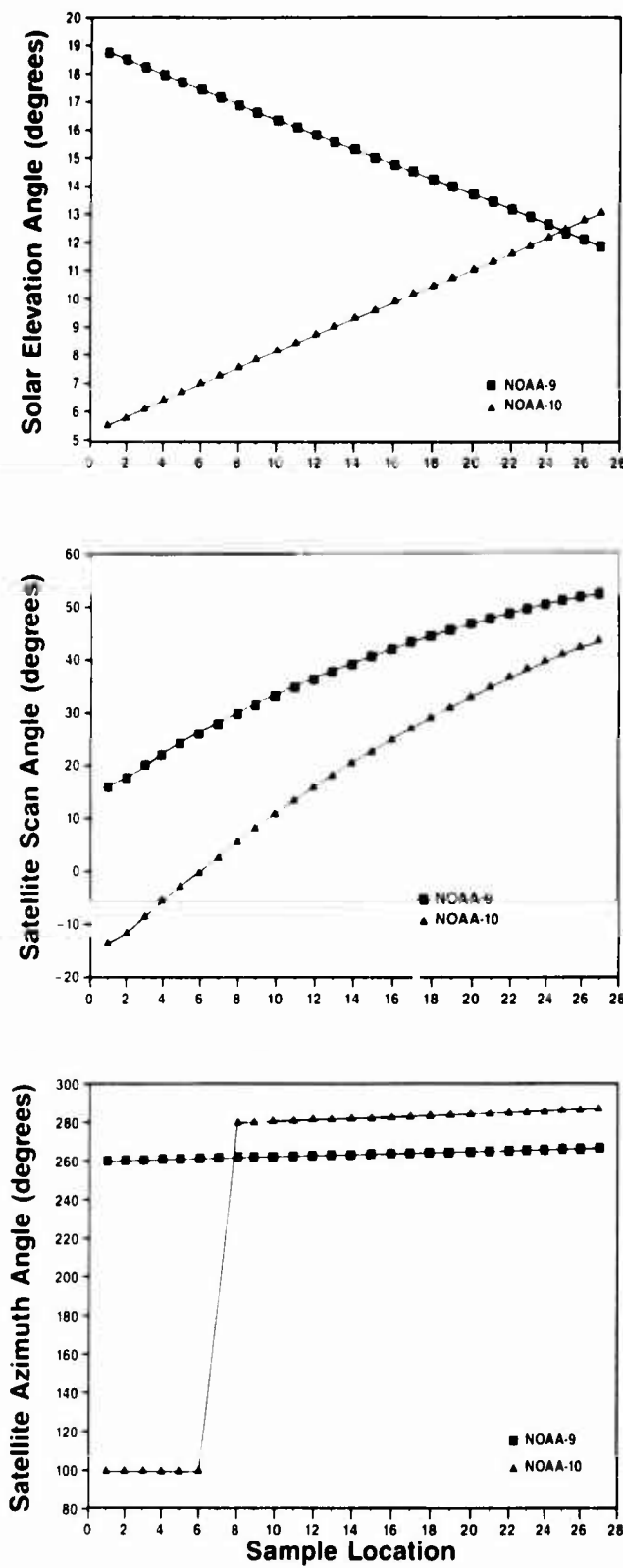


FIG. 2. Solar elevation angles and satellite scan and azimuth angles (south = 180°) for the sample locations of the northern transect of the study. Positive scan angles indicate scan in easterly direction.

38 are viewed from the west. NOAA-10 viewed locations 28 through 36 from the east, and locations 37 and 38 from the west.

Solar elevation above the horizon decreases at sample locations 1 through 27 for the NOAA-9 data (Figure 2), while it in-

creased for the NOAA-10 data. Solar elevation angles varied less between the two satellites for data acquired along the southern transect.

Solar azimuth angles (not shown) varied little over the two transects, with the sun positioned southwest of the sample locations at the time of the NOAA-9 orbit, and east-southeast of the locations at the time of the NOAA-10 orbit.

DIFFERENCES IN THE VISIBLE AND NEAR-IR RESPONSES OF THE SENSORS

The visible and near-IR response of both AVHRR sensors (Figure 3) tended to increase, from west to east, along the northern transect. NOAA-9 visible and near-IR response was greater than NOAA-10 response at all locations of the northern transect except locations 27. Sample location 27 was positioned in the Atlantic Ocean (Figure 1).

The increases and decreases in visible and near-IR response, from location to location, were similar for the two satellites. The amplitude of these fluctuations was greater for the NOAA-9 data from locations 1 through 19.

Locations 1 through 26 as viewed by NOAA-9 and locations 12 through 26 as viewed by NOAA-10 displayed a trend of increased visible and near-IR response for progressively eastward locations (Figure 3). This trend appears related to increased scan angles of the satellites and the associated increase in the amount of the Earth's atmosphere between the satellite and Earth's surface. The NOAA-10 visible and near-IR response did not exhibit the trend observed in the NOAA-9 for locations 1 through 12. Visible and near-IR data presented by Duggin *et al.* (1982), for the central United States centered on Illinois, displayed little variation between $\pm 14^\circ$ scan angles. The scan angles of the NOAA-10 satellite for these locations ranged from -13.7 to 13.5 degrees. The satellite scan angles at these locations for the NOAA-9 views ranged from 15.8 degrees at location 1 to 37.1 degrees at location 12.

Stimulated NOAA-7 AVHRR measurements of bidirectional reflectance (Holben *et al.*, 1986) indicated that near-IR and visible reflectance will vary when viewed at large scan angles. Holben *et al.* (1986) also found that simulated reflectance was greater from the backward scatter view (view away from direction of sun) as opposed to forward scatter direction. The NOAA-10 view of the northern transect east of location 6 would be considered a forward scatter direction while the NOAA-9 view would be considered backward scatter. The difference between the NOAA-9 and NOAA-10 visible response (Figure 3) is nearly constant with increased scan angles from sample locations 12 through 25. A slight decrease in the NOAA-9 and NOAA-10 near-IR response difference occurs with increased scan angles up to location 25 (Figure 3). The solar elevation angle differences between the satellites (Figure 2) decreased from 5 degrees at location 16 to essentially no difference at location 25. These results indicate that the forward scatter view (the view of NOAA-10) has a relatively greater near-IR response at the large scan angles and locations viewed in this study.

The visible and near-IR responses for the two satellite views along the southern transect fluctuated; though they still displayed similar patterns (Figure 4). The data for site 28 were excluded from subsequent analysis due to possible cloud contamination of the NOAA-9 data. Climatological Data for Baton Rouge, Louisiana (identified as "K" in Figure 1) indicated a sky cover of 80 percent near the time of the NOAA-9 data acquisition. This was the only sample location judged, through visual examination of the images or through climatological data, to have cloud contamination and excluded from further analysis.

Similar to the results of the northern transect, NOAA-9 visible and near-IR response for the southern transect was greater than that of NOAA-10. The trend exhibited in the northern transect

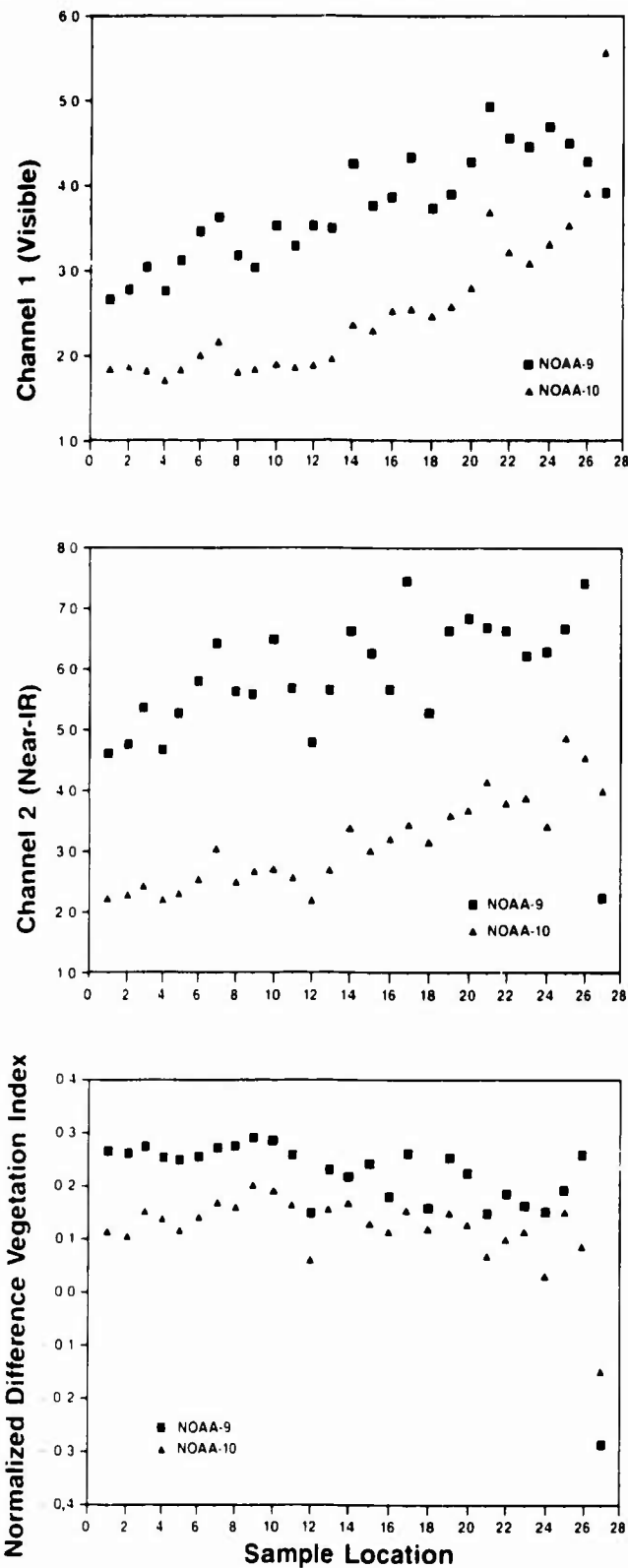


FIG. 3. Visible (percent), near-IR (percent), and normalized difference response for the sample locations of the northern transect of the study.

of increased visible and near-IR values with increased scan angles was not apparent for the southern transect. The visible response of NOAA-9 exhibited a slight (location 35 excluded) increase with increased scan angle for locations 30 through 38 in the backscatter

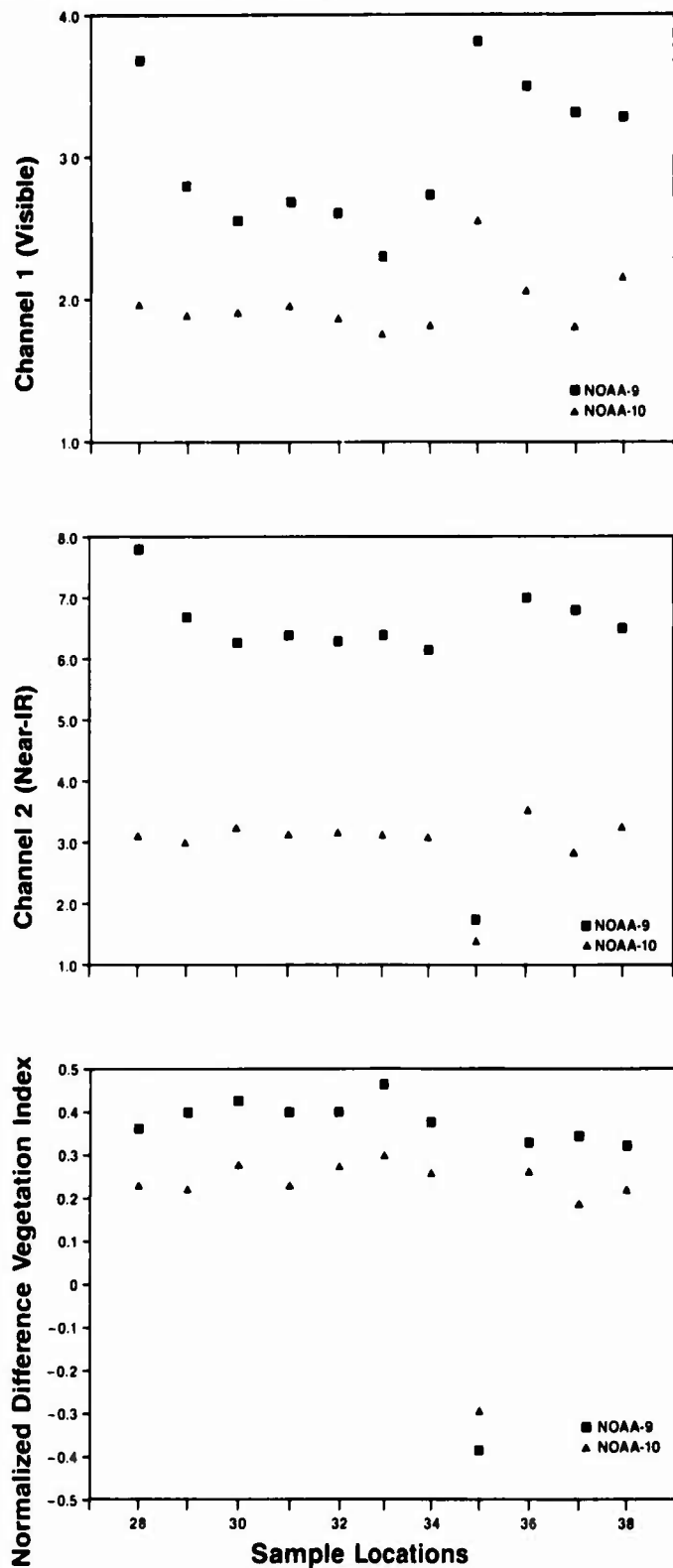


FIG. 4. Visible (percent), near-IR (percent), and normalized difference response for the sample locations of the southern transect of the study.

direction. The scan angle for the NOAA-9 view of location 38 was 22.4 degrees. The greatest satellite scan angle along the southern transect was 23.2 degrees for the NOAA-10 view of location 28. The NOAA-10 data at location 28 were not judged (through visual examination of the image and through climatological data) to have cloud contamination. Only a slight

increase in NOAA-10 visible is displayed from location 34 through 28 in the backward scatter direction. This increase may be due to changes in the surface reflectance as the NOAA-9 visible response also increases while scan angles decrease from 12.8 degrees at location 34 to 0.8 degrees at location 29.

DIFFERENCES IN THE VEGETATION INDICES OF THE SENSORS

The normalized difference vegetation indices computed for the locations along the northern transect (Figure 1) were all larger for the NOAA-9 data compared to NOAA-10, except at sample location 27. This result is similar to that for the individual channels. While the individual channel data increased with progressively eastern sample locations, the ND (Figure 3) was fairly stable along the transect for each satellite. There appears to be a slight decrease in the ND (Figure 3) for the greater satellite scan angles of the progressively eastern land surface locations (up to location 26) of the transect. A portion of the decrease may be attributable to unsubstantiated changes in the land surface features along the transect; however, this result agrees with results observed for AVHRR normalized difference data by Duggin *et al.* (1982) and Taylor *et al.* (1985). Similar to the visible and near-IR response, the NOAA-9 and NOAA-10 vegetation index values display similar patterns of fluctuation along the transect although the amplitude of the fluctuation is greater for the NOAA-9 indices.

Similar to the results of the northern transect, NOAA-9 ND values (Figure 4) were greater than those of NOAA-10 along the southern transect (except for the sample that included water, location 35). The amplitude of the fluctuations was not as great as that observed along the northern transect.

VISIBLE, NEAR-IR, AND VEGETATION INDEX RELATIONSHIPS

The NOAA-9 visible and near-IR response and normalized difference values were evaluated with their corresponding NOAA-10 values for each sample location. A linear relationship ($F = 36.38$, $P \leq 0.001$; RMSE = 0.48) exists between the visible response values of the two satellites (Figure 5); however, NOAA-9 visible response increased from 2.4 to 3.4 with no apparent increase in NOAA-10 values. NOAA-10 values increase from approximately 2.5 to 5.5 with relatively little change in NOAA-9 values. The NOAA-10 visible response was associated with 77 percent of the variation in the NOAA-9 response ($F = 108.0$, $P \leq 0.001$; RMSE = 0.34) when the two water surface samples (sample locations 27 and 35) were excluded from the analysis.

The relationship between the near-IR response of the two sensors was also linear, however, more variable than that of the visible response ($F = 13.6$, $P \leq 0.001$; RMSE = 1.04). The near-IR response for the water surface locations range from 1.4 to 4.1 for NOAA-10; however, the range is only 1.7 to 2.1 for NOAA-9. The variation in the NOAA-10 near-IR response was associated with 59 percent of the variation in the NOAA-9 data ($F = 47.9$, $P \leq 0.001$; RMSE = 0.48) when the two water surface samples were excluded.

Linear relationships were evident between the vegetation index values of NOAA-9 and those of NOAA-10 (Figure 5). The NOAA-10 normalized difference index was associated with 92 percent of the variation in the NOAA-9 index ($F = 400.26$, $P \leq 0.001$; RMSE = 0.05). Although a linear relationship, the NOAA-9 values for a specific location were greater than those of NOAA-10 (except for the water surface locations). The gain and offset, derived from the data of this study, that would permit computation of NOAA-9 ND values from NOAA-10 values were 1.4 and 0.04, respectively.

CONCLUSIONS AND RECOMMENDATIONS

The results of this study indicate that for land surface features the NOAA-9 satellite data included greater visible and near-IR

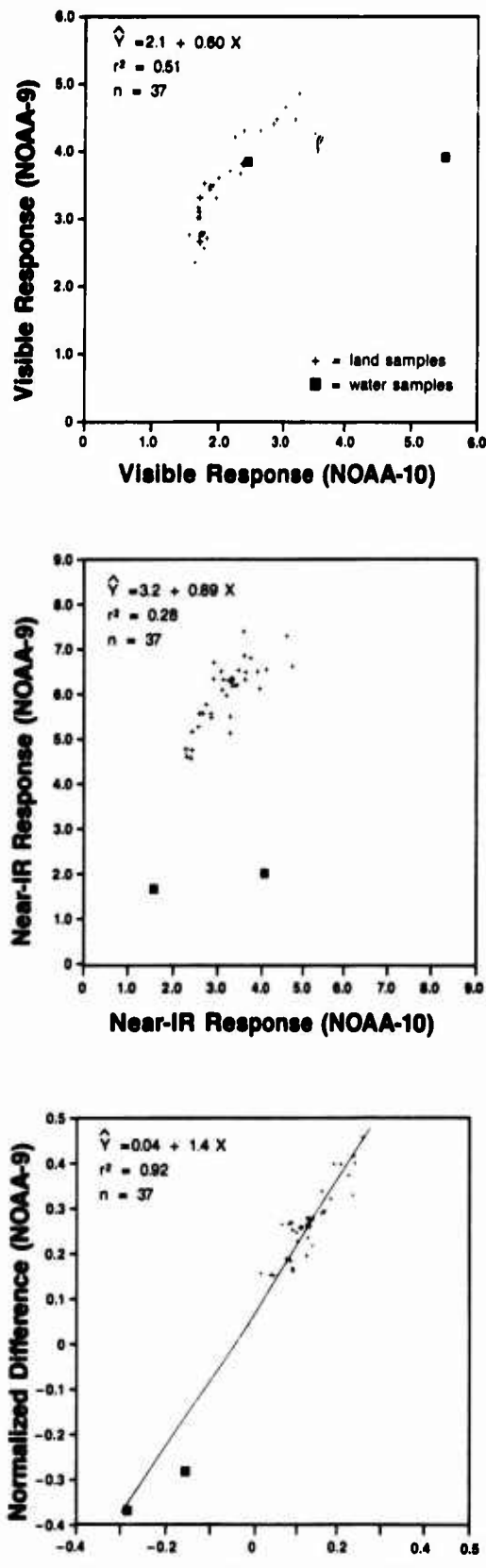


Fig. 5. Visible (percent), near-IR (percent), and normalized difference response of the NOAA-9 AVHRR compared to the NOAA-10 AVHRR (location 28 was excluded). The fitted regression line is for the relationship between the normalized difference computed from NOAA-9 and NOAA-10 data.



response values compared to NOAA-10 data. These greater responses were observed even when the solar elevation angles were nearly equal at the sampled locations viewed by the two satellites.

The results of this study, as also reported by others, indicate that visible and near-IR responses increase with increased satellite scan angles for land surface features. The vegetation indices, as expected from the results of prior studies, were not influenced by increased scan angles as greatly as the visible or near-IR response. There appeared to be a slight decrease in the ND vegetation index with progressively larger scan angles.

The NOAA-10 visible and near-IR response were associated with less of the variability in the NOAA-9 visible and near-IR response compared to a vegetation index computed from the data. This result supports the use of a vegetation index, compared to individual channel responses, for multisensor assessments of land surfaces.

The normalized difference vegetation index appears to be a simple method of making relative assessments of land surface features with AVHRR data acquired from either a morning or afternoon orbit. This index, with an appropriate gain and offset, may also be a method for utilizing the data of a NOAA AVHRR with a morning orbit as a substitute, when data are not available, for an afternoon orbit. Future studies might include evaluations of additional vegetation indices, as well as the normalized difference index.

Recommendations include further evaluation of the similarities and differences between the data of the morning and afternoon orbits under varied and similar when possible solar illumination, satellite view angles, and surface feature conditions. Future studies might include evaluations of additional vegetation indices as well as the normalized difference index. The utilization of these data as input to, or as verification of, models may result in a confident estimate of the AVHRR visible, near-IR, or vegetation index response for an afternoon orbit with data acquired from a morning orbit.

REFERENCES

Asrar, G., M. Fuchs, E. T. Kanemasu, and J.L. Hatfield, 1984. Estimating absorbed photosynthetic radiation and leaf area index from spectral reflectance in wheat, *Agron. J.* 76:300-306.

Brown, R. J., M. Bernier, and G. Fedosejevs, 1982. Geometrical and atmospheric considerations of NOAA AVHRR imagery, *Proc. of the 8th International Symposium on Machine Processing of Remotely Sensed Data*, Purdue University, West Lafayette, Indiana, pp. 374-381.

Daughtry, C. S. I., K. P. Gallo, and M. E. Bauer, 1983. Spectral estimates of solar radiation intercepted by corn canopies, *Agron. J.* 75:527-531.

Duggin, M. L., D. Piwinski, V. Whitehead, and G. Ryland, 1982. Evaluation of NOAA-AVHRR data for crop assessment, *Applied Optics* 21:1873-1875.

Dusek, D. A., R. D. Jackson, and J. T. Musick, 1985. Winter wheat vegetation indices calculated from combination of seven spectral bands, *Remote Sens. Environ.* 18:255-267.

Gallo, K. P., C. S. I. Daughtry, and M. E. Bauer, 1985. Spectral estimation of absorbed photosynthetically active radiation in corn canopies, *Remote Sens. Environ.* 17:221-232.

Gallo, K. P., and C. S. I. Daughtry, 1987. Differences in vegetation indices for simulated Landsat-5 MSS and TM, NOAA-9 AVHRR, and SPOT-1 sensor systems, *Remote Sens. Environ.* 23:439-452.

Gardner, B. R., B. L. Blad, D. R. Thompson, and K. E. Henderson, 1985. Evaluation and interpretation of thematic mapper ratios in equations for estimating corn growth parameters, *Remote Sens. Environ.* 18:225-234.

Goward, S. N., C. J. Tucker, and D. G. Dye, 1985. North American vegetation patterns observed with the NOAA-7 advanced very high resolution radiometer, *Vegetatio* 64:3-14.

Hatfield, J. L., G. Asrar, and E. T. Kanemasu, 1984. Intercepted photosynthetically active radiation estimated by spectral reflectance, *Remote Sens. Environ.* 14:65-75.

Hatfield, J. L., E. T. Kanemasu, G. Asrar, R. D. Jackson, P. J. Pinter, Jr., R. J. Reginato, and S. B. Idso, 1985. Leaf-area estimates from spectral measurements over various planting dates of wheat, *Int. J. Remote Sens.* 6:167-175.

Hinzman, L. D., M. E. Bauer, and C. S. T. Daughtry, 1986. Effects of nitrogen fertilization on growth and reflectance characteristics of winter wheat, *Remote Sens. Environ.* 19:47-61.

Holben, B. N., 1986. Characteristics of maximum-value composite images from temporal AVHRR data, *Int. J. Remote Sens.* 7:1417-1434.

Holben, B., and R. S. Fraser, 1984. Red and near-infrared sensor response to off-nadir viewing, *Int. J. Remote Sens.* 5:145-160.

Holben, B., D. Kimes, and R. S. Fraser, 1986. Directional reflectance response in AVHRR red and near-IR bands for three cover types and varying atmospheric conditions, *Remote Sensing of Environ.* 19:213-236.

Jackson, R. D., P. N. Slater, and P. J. Pinter, Jr., 1983. Discrimination of growth and water stress in wheat by various vegetation indices through clear and turbid atmospheres, *Remote Sensing of Environ.* 13:187-208.

Justice, C. O. (ed.), 1986. Monitoring the Grasslands of Semi-arid Africa using NOAA AVHRR Data, Special Issue: *Int. J. Remote Sensing*, 5:1383-1622.

Justice, C. O., J. R. G. Townshend, B. N. Holben, and C. J. Tucker, 1985. Analysis of the phenology of global vegetation using meteorological satellite data, *Int. J. Remote Sens.* 6:1271-1318.

Kidwell, K. B., 1986. *NOAA Polar Orbiter Data (TIROS-N, NOAA-6, NOAA-7, NOAA-8, NOAA-9, and NOAA-10) Users Guide*. National Oceanic and Atmos. Admin., U.S. Dept. Comm., Washington, D.C. 20233.

Schneider, S. R., D. F. McGinnis, Jr., and G. Stephens, 1985. Monitoring Africa's Lake Chad basin with LANDSAT and NOAA satellite data, *Int. J. Remote Sens.* 6:59-73.

Tarpley, J. D., S. R. Schneider, and R. L. Money, 1984. Global vegetation indices from NOAA-7 meteorological satellite, *J. Climate and Appl. Meteor.* 23:491-493.

Taylor, B. F., P. W. Dini, and J. W. Kidson, 1985. Determination of seasonal and interannual variation in New Zealand pasture growth from NOAA-7 data, *Remote Sensing of Environ.* 18:177-192.

Tucker, C. J., I. Y. Fung, C. D. Keeling, and R. H. Gammon, 1986. Relationship between atmospheric CO₂ variations and a satellite-derived vegetation index, *Nature* 319:195-199.

Tucker, C. J., J. R. G. Townshend, and T. E. Goff, 1985. African land-cover classification using satellite data, *Science* 227:369-375.

U.S. Department of Agriculture, Soil Conservation Service, 1981. *Land Resource Regions and Major Land Resource Areas of The United States*. Agriculture Handbook 296, Revised 1981. U.S. Government Printing Office, Washington, D.C.

Young, T. L., and J. H. Fahle, 1981. *User's Manual for Preliminary Satellite Image Processing: Extraction, Calibration, and Location*. Scripps Institution of Oceanography (SIO) reference no. 81-36, Univ. of California-San Diego, La Jolla, California, 200 p.

(Received 3 August 1987; revised and accepted 7 December 1987)

Please Tell Our Advertisers You Saw Their Ad in
PE&RS